

**Measurement of neutron multiplicity from fission of  $^{228}\text{U}$  and nuclear dissipation**

Hardev Singh,<sup>\*</sup> B. R. Behera, Gulzar Singh, and I. M. Govil  
*Department of Physics, Panjab University, Chandigarh 160014, India*

K. S. Golda, Akhil Jhingan, R. P. Singh, P. Sugathan, M. B. Chatterjee, and S. K. Datta  
*Inter University Accelerator Centre, New Delhi 110067, India*

Santanu Pal  
*Variable Energy Cyclotron Centre, 1/AF, Bidhan Nagar, Kolkata 700064, India*

Ranjeet and S. Mandal  
*Department of Physics and Astrophysics, Delhi University, Delhi 110007, India*

P. D. Shidling<sup>†</sup>  
*Department of Physics, Karnatak University, Dharwad 580003, India*

G. Viesti  
*Dipartimento di Fisica and Sezione INFN Padova, I-35131 Padova, Italy*  
 (Received 3 November 2009; published 30 December 2009)

Pre- and post-scission neutron multiplicities are measured at different excitation energies of the compound nucleus  $^{228}\text{U}$  populated using the  $^{19}\text{F} + ^{209}\text{Bi}$  reaction. The measured yield of pre-scission and total neutrons are compared with the statistical model calculation for the decay of a compound nucleus. The statistical model calculations are performed using the Bohr-Wheeler transition state fission width as well as the dissipative dynamical fission width due to Kramers. Comparison between the measured and the calculated values shows that, while the Bohr-Wheeler fission width grossly underestimates the pre-scission neutron yield, a large amount of dissipation is required in the Kramers width to fit the experimental pre-scission multiplicities. Various factors contributing to the large excitation energy dependence of the fitted values of the dissipation coefficient are discussed.

DOI: [10.1103/PhysRevC.80.064615](https://doi.org/10.1103/PhysRevC.80.064615)

PACS number(s): 25.70.Jj, 25.70.Gh, 24.10.Pa

**I. INTRODUCTION**

The goal of synthesizing super-heavy elements and the urge to understand the underlying reaction mechanism have initiated a large number of experimental and theoretical studies in the dynamics of bulk nuclear matter in heavy-ion-induced fusion-fission reaction [1–5]. A detailed understanding of the fusion-fission reaction dynamics is necessary for a judicious selection of target-projectile combinations for the production of super-heavy nuclei. A number of experimental probes have been developed to investigate the reaction mechanism of nucleus-nucleus collisions at energies above the Coulomb barrier. The systematic study of the experimentally observed pre-scission multiplicity of light particles (both neutrons and charged particles) and that of giant dipole resonance (GDR)  $\gamma$  rays, evaporation residue cross section, and the mass and angular distribution of fission fragments are now well established tools to study the fusion-fission dynamics induced by heavy ions [6–13]. Extensive measurements using the

aforementioned tools strongly suggest the dissipative nature of nuclear dynamics at high excitation energies as was suggested by Thoennessen and Bertsch [14] earlier.

In the fission of a heavy compound nucleus at an excitation energy of a few tens of MeV or higher, it is observed [15,16] that the number of pre-scission neutrons emitted is much larger than that predicted by the transition-state fission model due to Bohr and Wheeler [17]. Thus, a dissipative dynamical model becomes more appropriate for fission of highly excited nuclei. Dissipative dynamics slows down the fission process and consequently a larger number of neutrons can be evaporated than that allowed by the transition-state model. Pre-scission neutrons can be emitted in a number of stages in a fusion-fission reaction. The dinuclear complex in the entrance channel evolves over a certain duration of time before a fully equilibrated compound nucleus (CN) is formed. Energy equilibration being a fast process [18], the system is fully energy equilibrated during this time interval while it essentially relaxes in the shape degrees of freedom during this formation time period. Neutrons can thus be emitted during the formation period of the CN and contribute to the total number of pre-scission neutrons. The formation time can be large, in particular, for systems with an entrance channel mass asymmetry,  $\alpha = (A_t - A_p)/(A_t + A_p)$ , smaller than the critical Businaro-Gallone mass asymmetry,  $\alpha_{BG}$ , for the CN.

<sup>\*</sup>Present address: Department of Chemistry, University of Rochester, Rochester, NY 14627, USA.

<sup>†</sup>Present address: Kernfysisch Versneller Instituut, Zernikelaan 25, NL-9747 AA Groningen, The Netherlands.

A large-scale mass rearrangement takes place during fusion of such systems requiring a relatively longer period of time [8]. The equilibrated CN can subsequently undergo fission, which can be considered as a quasi-stationary diffusion process over the fission barrier. The steady-state fission rate was obtained by Kramers [19] and nuclear dissipation plays an important role at this stage. The number of neutrons emitted during this stage when the CN evolves from its ground-state configuration to the saddle shape makes the largest contribution to the multiplicity of pre-scission neutrons. After the CN crosses the saddle point, another time interval elapses before it reaches the scission point and the CN can continue emitting neutrons during this interval and thus make an additional contribution to the number of pre-scission neutrons. The saddle-to-scission dynamics is also controlled by the dissipative force.

The average number of neutrons emitted during the ground state to the saddle transition is usually obtained with the statistical model of nuclear decay. The number of neutrons emitted during saddle-to-scission transition can also be obtained from the elapsed time interval [20]. The dissipation strength is treated as a free parameter in these calculations. The number of neutrons emitted during the formation time is not usually calculated separately because it requires an entrance channel dynamical calculation in a multidimensional potential landscape. Therefore, when the dissipation strength is adjusted to fit the calculated number of neutrons with the experimental data, it also has to account for the neutrons emitted during the formation time. Further, for highly fissile CN, the time required to establish a steady flow can often be comparable with the fission lifetime itself [21]. In such cases, a substantial number of fission events can take place during the transient period. Because transient effects are included in the statistical model calculations in an approximate manner, the dissipation coefficient also has to partly account for the transient effects.

It would be of interest, therefore, to study the neutron multiplicity of a highly fissile CN formed in an entrance channel with  $\alpha < \alpha_{BG}$  to investigate the nature of the dissipation coefficient required to fit the data. With this objective, we have measured the neutron multiplicities from  $^{228}\text{U}$  (with fissility parameter  $x = 0.782$  and  $\alpha_{BG} = 0.879$ ) formed in the  $^{19}\text{F} + ^{209}\text{Bi}$  reaction with asymmetry  $\alpha = 0.833$ , thus making  $\alpha < \alpha_{BG}$ . The measurements are carried out at  $E_{\text{lab}} = 100, 104, 108, 112, \text{ and } 116$  MeV. Subsequently we perform detailed statistical model calculations to fit the experimental data. The experimental details are given in the next section. Section III contains a brief description of the extraction of the pre-scission and total neutron multiplicities from the experimental data. The details of the statistical model calculations are given in Sec. IV. The work is summarized in the last section.

## II. EXPERIMENTAL DETAILS

The experiment was performed using a pulsed beam of  $^{19}\text{F}$  obtained from the 15UD Pelletron of the Inter University Accelerator Centre (IUAC), New Delhi. A self-supporting target of  $^{209}\text{Bi}$  of  $350 \mu\text{g}/\text{cm}^2$  in thickness was used. The fission-neutron coincidence technique was used to collect the

event-by-event mode data. Four liquid scintillator neutron detectors of dimension  $5 \times 5''$  were used for the detection of neutrons. The detectors were placed outside the scattering chamber at angles of  $30^\circ, 60^\circ, 90^\circ, \text{ and } 120^\circ$  with respect to the beam direction and at a distance of 100 cm from the target. Thin flanges of 3-mm stainless steel (SS) were used with the scattering chamber to minimize neutron scattering. The neutron detector array threshold was kept at about 120 keVee by calibrating it with standard  $\gamma$  sources ( $^{137}\text{Cs}$  and  $^{60}\text{Co}$ ) [22].

Two large-area ( $20 \times 10$  cm) position-sensitive multiwire proportional counters (MWPC) [23] were placed at the folding angle for symmetric fission. Detectors were placed on movable arms on both sides of the beam at distances/angles of 60 cm ( $90^\circ$ ) and 50 cm ( $65^\circ$ ), respectively, from the target. The small variation in the folding angle with the beam energy was corrected by moving one of the gas detectors placed at  $65^\circ$ . Beam flux monitoring as well as normalization was done using the elastic events collected by two silicon surface barrier detectors placed at  $\pm 10^\circ$ . The event collection was triggered by the detection of a fission fragment in any of the gas detectors. The details of the experimental setup are given in Refs. [24,25]. To keep the background in time-of-flight (TOF) spectra at the minimum level, the beam dump was kept at 3 m from the target and was well shielded with layers of lead and borated paraffin. Discrimination between neutrons and  $\gamma$ 's was made by using pulse shape discrimination (PSD) based on the zero cross technique [26] and TOF. The neutron TOF was converted into neutron energy using prompt  $\gamma$  peak in TOF spectrum as time reference. The efficiency correction for the neutron detectors was done using the Monte Carlo computer code MODEFF [27]. The Monte Carlo calculations, in turn, were verified by measuring the relative efficiency of the detector using a  $^{252}\text{Cf}$  spontaneous fission source [28].

## III. DATA ANALYSIS

The three components (pre-scission from CN and post-scission from the two accelerated fission fragments) of neutron multiplicities were obtained by fitting the fission neutron angular correlations using a multiple-source fitting procedure [29]. The neutron emissions from these moving sources were assumed to be isotropic in their respective rest frames. Thus, the measured double-differential neutron multiplicities are given as

$$\frac{d^2 M_n}{dE_n d\Omega_n} = \sum_{i=1}^3 \frac{M_{n_i} \sqrt{E_n}}{2(\pi T_i)^{3/2}} \times \exp\left(-\frac{E_n - 2\sqrt{E_n E_i/A_i} \cos \theta_i + E_i/A_i}{T_i}\right). \quad (1)$$

Here,  $E_n$  is the laboratory energy of the neutron and  $E_i$ ,  $T_i$ , and  $M_{n_i}$  represent energy, temperature, and multiplicity of each neutron emission source.  $A_i$  is the mass of each neutron source and  $\theta_i$  represents the relative angle between the neutron direction and the source direction. The folding angles were obtained from the systematics of Viola *et al.* [30]

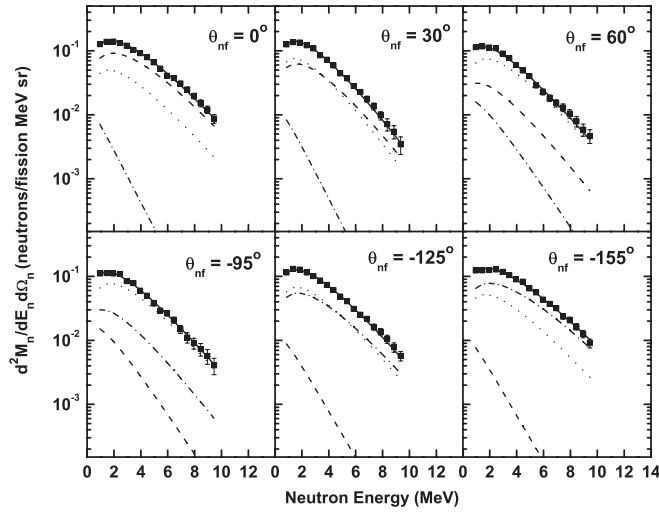


FIG. 1. Neutron multiplicity spectra (solid squares) for the  $^{19}\text{F} + ^{209}\text{Bi}$  reaction at  $E_{\text{lab}} = 108$  MeV along with the fits for the pre-scission (dotted curve) and the post-scission from fragment 1 (dashed curve) and fragment 2 (dot dashed curve). The solid curve represents the total contribution.

for symmetric fission. The angular acceptance of the neutron detectors and the fission detectors was taken into account in the fitting procedure. Figure 1 shows the fits to the double-differential neutron multiplicity spectra at various angles. The post-scission multiplicity and the temperatures were assumed to be the same for both the fission fragments, and the total multiplicity was derived as  $M_n^{\text{tot}} = M_n^{\text{pre}} + 2M_n^{\text{post}}$ .

#### IV. STATISTICAL MODEL ANALYSIS

The measured values of neutron multiplicities were compared with the statistical model predictions. In the statistical model calculation, in addition to fission, emission of light particles (neutron, proton, and  $\alpha$ ) and GDR  $\gamma$  rays were considered as decay channels for an excited compound nucleus. The light particle and GDR  $\gamma$ -ray partial widths were obtained from the Weisskopf formula [31]. The neutron multiplicities were first calculated using the following transition-state fission width due to Bohr and Wheeler [17],

$$\Gamma_{\text{BW}} = \frac{1}{2\pi\rho_g(E_i)} \int_0^{E_i - V_B} \rho_s(E_i - V_B - \epsilon) d\epsilon, \quad (2)$$

where  $\rho_g$  is the level density at the initial state and  $\rho_s$  is the level density at the saddle point. The spin-dependent fission barrier,  $V_B$ , is calculated from the finite-range liquid drop model for the nuclear potential [32] and the rigid rotator values of the moment of inertia. The level density parameter was taken from the works of Reisdorf [33] and is given as follows,

$$a(U) = \tilde{a} \left( 1 + \frac{f(U)}{U} \delta W \right), \quad (3)$$

$$f(U) = 1 - \exp(-U/E_D),$$

where  $U$  is the thermal energy of the CN,  $\delta W$  is the shell correction taken from the difference between the experimental

and the liquid drop model masses,  $E_D$  accounts for the rate at which the shell effect melts away with increase of excitation energy and  $\tilde{a}$  is the asymptotic value to which the level density parameter approaches with increasing excitation energy of the CN. The asymptotic level density parameter  $\tilde{a}$  depends upon the nuclear mass, shape, and pairing energy in a fashion similar to that of the liquid drop mass [33]. In addition to the excitation energy dependence, a temperature dependence of the level density parameter was also included in the calculation [34] and the final form of the level density parameter is given as

$$a(T) = a(U)[1 - \kappa f(T)], \quad (4)$$

$$f(T) = 1 - \exp[-(TA^{1/3}/21)^2],$$

where  $a(U)$  is calculated according to Eq. (3) and  $\kappa$  determines the strength of the additional temperature dependence.  $\kappa$  in the range of 0.4–0.8 was used in earlier works [10]. We have used  $\kappa = 0$  and 0.8 in the present calculation.

In the transition-state model, fission is considered to have taken place when the CN crosses the saddle point deformation. During transition from saddle to scission, the CN can emit more neutrons, which contribute to its pre-scission multiplicity. The saddle-to-scission time interval is given as

$$\tau_{\text{ssc}} = \tau_{\text{ssc}}^0 [(1 + \gamma^2)^{1/2} + \gamma]. \quad (5)$$

Here, the dimensionless dissipation parameter  $\gamma$  is related to the reduced dissipation coefficient  $\beta$  by  $\gamma = \beta/2\omega_s$ , where,  $\omega_s$  describes the saddle point curvature.  $\tau_{\text{ssc}}^0$  is the nondissipative saddle-to-scission time and its value is given as [35]

$$\tau_{\text{ssc}}^0 = \frac{2}{\omega_0} R[(\Delta V/T)^{1/2}], \quad (6)$$

where

$$R(z) = \int_0^z \exp(y^2) dy \int_y^\infty \exp(-x^2) dx, \quad (7)$$

and  $\Delta V$  is the potential energy difference between the saddle and scission points. Using the above saddle-to-scission time interval, we have calculated the number of neutrons emitted during this period.

Using the aforementioned partial widths, the time evolution of a CN was followed in the statistical model code [36,37] till either fission occurred or an evaporation residue was formed. In the case of a fission event, the neutrons emitted during the saddle-to-scission transition were also treated as pre-scission neutrons. The multiplicity of neutrons emitted from the fission fragments (post-scission neutrons) was also calculated assuming a symmetric fission. The spin distribution of the CN was assumed to follow the usual Fermi distribution, the parameters ( $l_c$  and  $\delta l$ ) of which were fixed by fitting the experimental fusion cross sections [38]. The comparison of experimental pre-scission and total neutron multiplicities with the values predicted by the Bohr-Wheeler fission width using different values of  $\kappa$  is shown in Fig. 2. The comparison clearly shows that Bohr-Wheeler fission width grossly underestimates the measured pre-scission neutron yield at all energies even after incorporating the temperature dependence of the level density parameter.

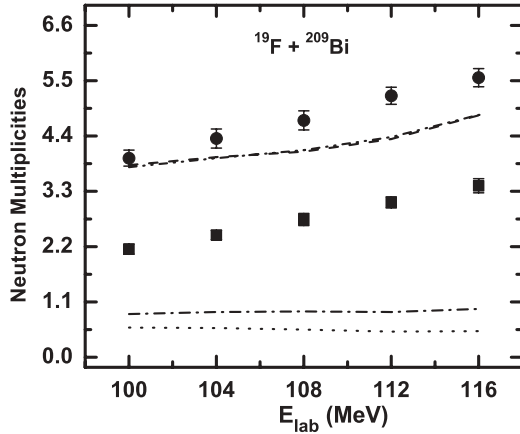


FIG. 2. Experimental pre-scission (solid squares) and total neutron multiplicities (solid circles) along with the values based on Bohr-Wheeler fission width for different values of  $\kappa$ . Dotted ( $\kappa = 0$ ) and dash-dotted ( $\kappa = 0.8$ ) lines represent the pre-scission values, whereas dashed ( $\kappa = 0$ ) and dash-double-dotted ( $\kappa = 0.8$ ) lines represent calculated total neutron multiplicities.

We next considered the Kramers stationary fission width [19],

$$\Gamma_K = \frac{\hbar\omega_g}{2\pi} e^{-V_B/T} \left\{ \sqrt{1 + \left(\frac{\beta}{2\omega_s}\right)^2} - \frac{\beta}{2\omega_s} \right\}, \quad (8)$$

where,  $\omega_g$  and  $\omega_s$  are the frequencies of the harmonic oscillator potentials that oscillate the liquid drop model nuclear potential at the ground-state and saddle configurations, respectively. Usually constant values are used for  $\omega_g$  and  $\omega_s$  and  $\gamma = \beta/2\omega_s$  is used as the free parameter in statistical model calculations [10]. However, it has recently been shown that  $\omega_g$  and  $\omega_s$  depend upon the spin of the CN resulting in a spin dependence of  $\gamma$  [39,40]. Figure 3 shows the spin dependence of the

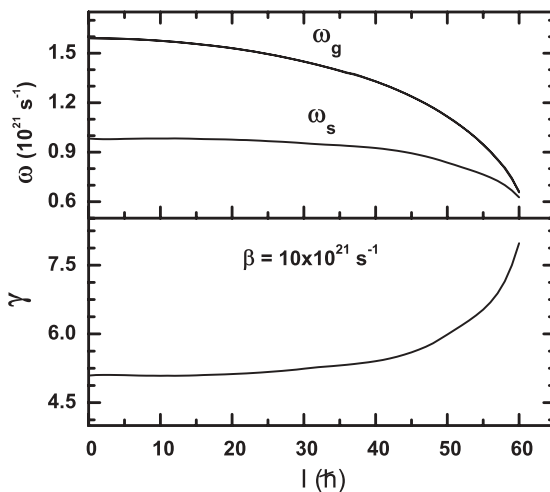


FIG. 3. Compound nuclear spin ( $l$ ) dependence of frequencies of harmonic oscillator potentials at ground state ( $\omega_g$ ), saddle point ( $\omega_s$ ), and dissipation parameter  $\gamma = \beta/2\omega_s$ .

frequencies and the dissipation parameter  $\gamma$ . Consequently, it would give rise to an energy dependence of  $\gamma$  because higher spin states of a CN are populated at higher excitation energies. We therefore choose  $\beta$  as the free parameter in the present calculation.

In a dissipative dynamical model of nuclear fission, the Kramers stationary width is reached after a buildup or transient time period given as [35,41]

$$\tau_{tr} = \beta/2\omega_g^2 \ln(10V_B/T). \quad (9)$$

The transient time is then incorporated into a dynamical fission width parametrized as

$$\Gamma_K(t) = [1 - \exp(-2.3t/\tau_{tr})]\Gamma_K, \quad (10)$$

which we have used in the evolution of a CN in the statistical model code.

To account for the neutrons emitted during the formation stage of the compound nucleus, we have introduced an interval  $t_{form}$  at the beginning of the time evolution in our calculation. No fission takes place during  $t_{form}$  though neutron and other particle evaporation channels are kept open. An estimate of  $t_{form} \approx 30 \times 10^{-21}$  s can be obtained from the systematic analysis of a large set of experimental data by Saxena *et al.* [8]. We have therefore used two different values of formation time ( $t_{form} = 0$  and 50 in units of  $\hbar/\text{MeV} = 0.66 \times 10^{-21}$  s) in our calculation.

The calculated pre-scission and total neutron multiplicities at different beam energies are shown in Fig. 4 along with the experimental data. No temperature dependence ( $\kappa = 0$ ) of the level density parameter is assumed in this calculation. It is observed that the energy dependence of the calculated pre-scission multiplicities for a given  $\beta$  is much smaller than

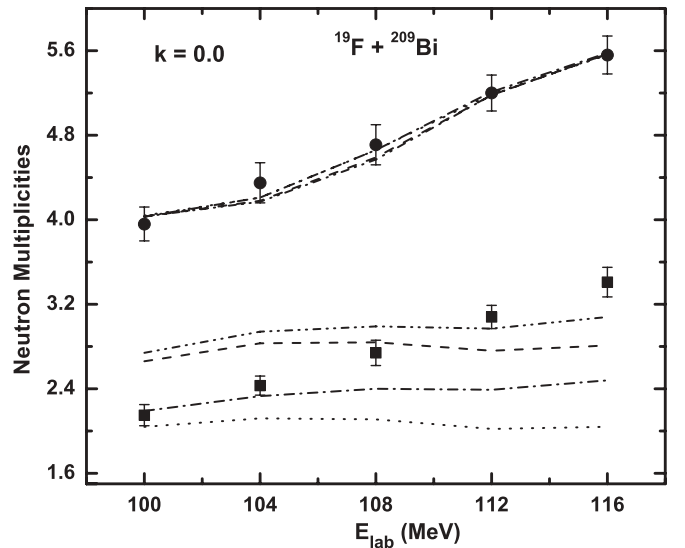


FIG. 4. Experimental pre-scission (solid squares) and total neutron multiplicities (solid circles) along with statistical model predictions for  $\kappa = 0$ . Dotted line,  $t_{form} = 0$ ,  $\beta = 4$ ; dashed line,  $t_{form} = 0$ ,  $\beta = 12$ ; dash-dotted line,  $t_{form} = 50$ ,  $\beta = 4$ ; and dash-double-dotted line ( $t_{form} = 50$ ,  $\beta = 12$ ).  $t_{form}$  and  $\beta$  are in units of  $\hbar/\text{MeV}$  and  $10^{21} \text{ s}^{-1}$ , respectively.

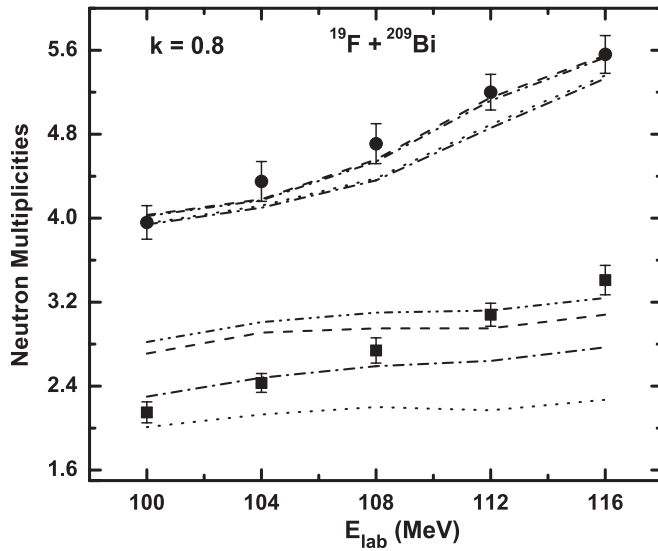


FIG. 5. Experimental pre-scission (solid squares) and total neutron multiplicities (solid circles) along with statistical model predictions with  $\kappa = 0.8$ . Dotted line,  $t_{\text{form}} = 0$ ,  $\beta = 1$ ; dashed line,  $t_{\text{form}} = 0$ ,  $\beta = 5$ ; dash-dotted line,  $t_{\text{form}} = 50$ ,  $\beta = 1$ ; and dash-double-dotted line,  $t_{\text{form}} = 50$ ,  $\beta = 5$ .  $t_{\text{form}}$  and  $\beta$  are in units of  $\hbar/\text{MeV}$  and  $10^{21} \text{ s}^{-1}$ , respectively.

that of the experimental values. This immediately suggests a strong energy dependence of  $\beta$  to fit the experimental values over the entire energy range. A similar observation is also made in Fig. 5 where the calculated multiplicities obtained with an energy dependence ( $\kappa = 0.8$ ) in the level density parameter are compared with the experimental data.

We have subsequently obtained the values of the reduced dissipation coefficient  $\beta$  that best fit the experimental pre-scission multiplicity at each beam energy separately. Figure 6 shows the initial excitation energy dependence of  $\beta$  for different values of  $\kappa$  and  $t_{\text{form}}$ . We also show the results where

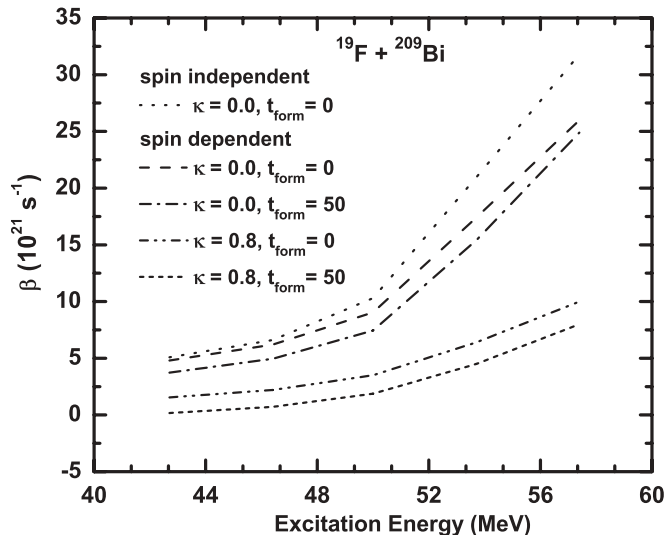


FIG. 6. Variation of best-fit  $\beta$  values for different values of  $\kappa$  and  $t_{\text{form}}$ .

spin-independent values of  $\omega_g$  and  $\omega_s$  are used. The values of the frequencies here are set equal to their zero spin values. We observe that the spin dependence of the frequencies results in a reduction in the magnitude and excitation energy dependence of the dissipation coefficient  $\beta$ . The introduction of a formation time further reduces the required values of the dissipation coefficient to fit the data. Moreover, a positive value of  $\kappa$  in Eq. (4) reduces the level density parameter and hence increases the CN temperature. Consequently, smaller values of  $\beta$  for  $\kappa = 0.8$  are required compared to those at  $\kappa = 0$  to give rise to the same number of pre-scission neutrons. This feature is also clearly observed in Fig. 6. A further reduction in  $\beta$  values is obtained when a formation time is considered along with  $\kappa = 0.8$ . We thus observe a substantial variation in the strength of the dissipation coefficient extracted from statistical model calculations depending upon the choice of different physical parameters. The issue of energy dependence of dissipation coefficient requires careful consideration because dissipation is a property of the nuclear bulk and mean-field theories of nuclear dissipation at temperature ranges considered here do not predict a strong temperature dependence of  $\beta$  [42]. Lestone and McCalla [43] have recently discussed in detail various features of the statistical model that have consequences in the extracted energy dependence of the dissipation coefficient. They have pointed out that the fission width in a statistical model calculation should include the effect of collective vibrations around the ground-state shape and the spin dependence of the frequencies  $\omega_g$  and  $\omega_s$ . Both have been incorporated in the present work. Reference [43] also considers the role of the orientation degree of freedom of the compound nucleus in determining the fission lifetime. Though the fission lifetime increases when the orientation degree of freedom is included in the calculation, it does not make any appreciable difference in the energy dependence of the fission lifetime. A temperature-dependent fission barrier is further introduced in the aforementioned work that, however, we have not considered here. This can have a bearing on the energy dependence of  $\beta$  that we find in Fig. 6.

## V. SUMMARY AND CONCLUSIONS

We have measured the pre- and post-scission neutron multiplicities from the fission of the  $^{228}\text{U}$  compound nucleus populated at various excitation energies using the  $^{19}\text{F} + ^{209}\text{Bi}$  reaction. The experimentally measured neutron multiplicities were compared with the statistical model predictions. The present results show that a dissipative fission dynamics is essential to explain the measured multiplicities of pre-scission neutrons.

An energy dependence in the fitted values of  $\beta$  is observed in the present work. The role of formation time of the CN and the spin dependence of the oscillator frequencies in reducing the energy dependence of  $\beta$  is demonstrated here. The energy dependence of  $\beta$  reduces further when a temperature dependence of the level density parameter is considered. More work is clearly required to settle the issue of the energy dependence of nuclear dissipation.

## ACKNOWLEDGMENTS

We are thankful to the accelerator group of IUAC for providing good quality pulsed beams. The help received from Mr. Abhilash in target preparation and Mr. P. Barua in setting up the experimental configuration in GPSC is gratefully

acknowledged. We are thankful to Dr. V. S. Ramamurthy for useful discussion on this work. We thank the Department of Science and Technology (DST), New Delhi, and the Council of Scientific and Industrial Research (CSIR), New Delhi, for financial support to carry out this work.

- 
- [1] D. J. Hinde, R. G. Thomas, R. du Rietz, A. Diaz-Torres, M. Dasgupta, M. L. Brown, M. Evers, L. R. Gasques, R. Rafiei, and M. D. Rodriguez, *Phys. Rev. Lett.* **100**, 202701 (2008).
- [2] L. R. Gasques, D. J. Hinde, M. Dasgupta, A. Mukherjee, and R. G. Thomas, *Phys. Rev. C* **79**, 034605 (2009).
- [3] D. J. Hinde, M. Dasgupta, and A. Mukherjee, *Phys. Rev. Lett.* **89**, 282701 (2002).
- [4] R. Yanez, D. J. Hinde, B. Bouriquet, and D. Duniec, *Phys. Rev. C* **71**, 041602(R) (2005).
- [5] V. S. Ramamurthy, S. S. Kapoor, R. K. Choudhury, A. Saxena, D. M. Nadkarni, A. K. Mohanty, B. K. Nayak, S. V. Sastry, S. Kailas, A. Chatterjee, P. Singh, and A. Naveen, *Phys. Rev. Lett.* **65**, 25 (1990).
- [6] H. Singh, K. S. Golda, S. Pal, Ranjeet, R. Sandal, B. R. Behera, G. Singh, A. Jhingan, R. P. Singh, P. Sugathan, M. B. Chatterjee, S. K. Datta, A. Kumar, G. Viesti, and I. M. Govil, *Phys. Rev. C* **78**, 024609 (2008).
- [7] J. Cabrera, T. Keutgen, Y. El Masri, C. Dufauquez, V. Roberfroid, I. Tilquin, J. V. Mol, R. Regimbart, R. J. Charity, J. B. Natowitz, K. Hagel, R. Wada, and D. J. Hinde, *Phys. Rev. C* **68**, 034613 (2003).
- [8] A. Saxena, A. Chatterjee, R. K. Choudhury, S. S. Kapoor, and D. M. Nadkarni, *Phys. Rev. C* **49**, 932 (1994).
- [9] J. P. Lestone, *Phys. Rev. Lett.* **70**, 2245 (1993).
- [10] I. Diószegi, N. P. Shaw, I. Mazumdar, A. Hatzikoutelis, and P. Paul, *Phys. Rev. C* **61**, 024613 (2000).
- [11] I. Diószegi, N. P. Shaw, A. Bracco, F. Camera, S. Tettoni, M. Mattiuzzi, and P. Paul, *Phys. Rev. C* **63**, 014611 (2000).
- [12] A. C. Berriman, D. J. Hinde, M. Dasgupta, C. R. Morton, R. D. Butt, and J. O. Newton, *Nature (London)* **413**, 144 (2001).
- [13] R. Tripathi, K. Sudarshan, S. Sodaye, A. V. R. Reddy, K. Mahata, and A. Goswami, *Phys. Rev. C* **71**, 044616 (2005).
- [14] M. Thoennessen and G. F. Bertsch, *Phys. Rev. Lett.* **71**, 4303 (1993).
- [15] D. Hilscher and H. Rossner, *Ann. Phys. (Paris)* **17**, 471 (1992).
- [16] D. J. Hinde, D. Hilscher, H. Rossner, B. Gebauer, M. Lehmann, and M. Wilpert, *Phys. Rev. C* **45**, 1229 (1992).
- [17] N. Bohr and J. A. Wheeler, *Phys. Rev.* **56**, 426 (1939).
- [18] W. U. Schroeder and J. R. Huizenga, *Treatise on Heavy-Ion Science*, edited by D. A. Bromley (Plenum, New York, 1984), Vol. 2, p. 115.
- [19] H. A. Kramers, *Physics (Amsterdam)* **7**, 284 (1940).
- [20] D. J. Hofman, B. B. Back, and P. Paul, *Phys. Rev. C* **51**, 2597 (1995).
- [21] G. Chaudhuri and S. Pal, *Eur. Phys. J. A* **14**, 287 (2002).
- [22] T. G. Masterson, *Nucl. Instrum. Methods* **88**, 61 (1970).
- [23] A. Jhingan, P. Sugathan, K. S. Golda, R. P. Singh, T. Varughese, H. Singh, B. R. Behera, and S. K. Mandal, *Rev. Sci. Instrum.* **80**, 123502 (2009).
- [24] H. Singh, A. Kumar, B. R. Behera, I. M. Govil, K. S. Golda, P. Kumar, A. Jhingan, R. P. Singh, P. Sugathan, M. Chatterjee, S. K. Datta, S. Pal, and G. Viesti, *Phys. Rev. C* **76**, 044610 (2007).
- [25] H. Singh, A. Kumar, B. R. Behera, G. Singh, I. M. Govil, K. S. Golda, P. Kumar, A. Jhingan, R. P. Singh, P. Sugathan, M. Chatterjee, S. K. Datta, Ranjeet, S. Pal, and G. Viesti, *Phys. Rev. C* **80**, 019909(E) (2009).
- [26] S. Venkataramanan, A. Gupta, K. Golda, H. Singh, R. Kumar, R. Singh, and R. Bhowmik, *Nucl. Instrum. Methods A* **596**, 248 (2008).
- [27] R. A. Cecil, B. D. Anderson, and R. Madey, *Nucl. Instrum. Methods* **161**, 439 (1979).
- [28] K. S. Golda, H. Singh, R. P. Singh, S. K. Datta, and R. K. Bhowmik, *National Symposium on Nuclear Physics* (2005), Vol. 50, p. 445.
- [29] D. Hilscher, J. R. Birkelund, A. D. Hoover, W. U. Schroeder, W. W. Wilcke, J. R. Huizenga, A. C. Mignerey, K. L. Wolf, H. F. Breuer, and V. E. Viola, *Phys. Rev. C* **20**, 576 (1979).
- [30] V. E. Viola, K. Kwiatkowski, and M. Walker, *Phys. Rev. C* **31**, 1550 (1985).
- [31] P. Frobrich and I. I. Gontchar, *Phys. Rep.* **292**, 131 (1998).
- [32] A. J. Sierk, *Phys. Rev. C* **33**, 2039 (1986).
- [33] W. Reisdorf, *Z. Phys. A* **300**, 227 (1981).
- [34] S. Shlomo and J. B. Natowitz, *Phys. Rev. C* **44**, 2878 (1991).
- [35] P. Grangé, S. Hassani, H. A. Weidenmuller, A. Gavron, J. R. Nix, and A. J. Sierk, *Phys. Rev. C* **34**, 209 (1986).
- [36] G. Chaudhuri and S. Pal, *Phys. Rev. C* **63**, 064603 (2001).
- [37] G. Chaudhuri and S. Pal, *Phys. Rev. C* **65**, 054612 (2002).
- [38] L. Pant, R. Choudhury, A. Saxena, and D. Biswas, *Eur. Phys. J. A* **11**, 47 (2001).
- [39] J. Sadhukhan and S. Pal, *Phys. Rev. C* **78**, 011603(R) (2008).
- [40] J. Sadhukhan and S. Pal, *Phys. Rev. C* **79**, 019901(E) (2009).
- [41] K. H. Bhatt, P. Grangé, and B. Hiller, *Phys. Rev. C* **33**, 954 (1986).
- [42] J. Blocki, Y. Boneh, J. R. Nix, J. Randrup, M. Robel, A. J. Sierk, and W. J. Swiatecki, *Ann. Phys.* **113**, 330 (1978).
- [43] J. P. Lestone and S. G. McCalla, *Phys. Rev. C* **79**, 044611 (2009).